Phase diagram of rotating QCD from lattice simulations with dynamical quarks

A. A. Roenko[1],

in collaboration with

V. V. Braguta[1], A. Yu. Kotov[2], D. A. Sychev[1,3]

[1]Joint Institute for Nuclear Research, Bogoliubov Laboratory of Theoretical Physics
[2]Jülich Supercomputing Centre
[3]Moscow Institute of Physics and Technology

"International Conference on Quantum Field Theory, High-Energy Physics, and Cosmology", BLTP JINR, 18-21 July 2022

JOINT INSTITUTE FOR NUCLEAR RESEARCH

Introduction

- In non-central heavy ion collisions creation of QGP with angular momentum is expected.

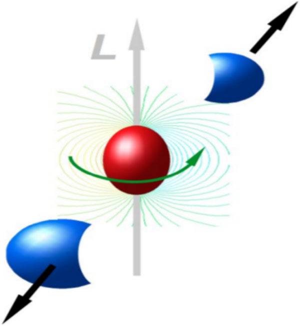

- In non-central heavy ion collisions creation of QGP with angular momentum is expected.
- The rotation occurs with relativistic velocities.

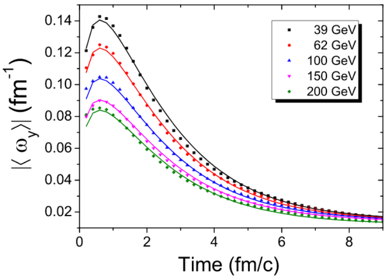

Au+Au, $b = 7$ fm

[Y. Jiang, Z.-W. Lin, and J. Liao, Phys. Rev. C **94**, 044910 (2016), arXiv:1602.06580 [hep-ph]]

$\omega \sim 0.1 - 0.2\,\mathrm{fm}^{-1} \sim 20 - 40$ MeV

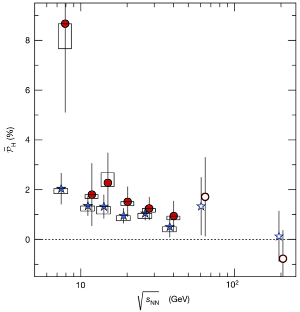

[L. Adamczyk et al. (STAR), Nature **548**, 62–65 (2017), arXiv:1701.06657 [nucl-ex]]

$\omega \sim 6$ MeV $\left(\sqrt{s_{NN}}\text{-averaged}\right)$

Introduction

- In non-central heavy ion collisions creation of QGP with angular momentum is expected.
- The rotation occurs with relativistic velocities.

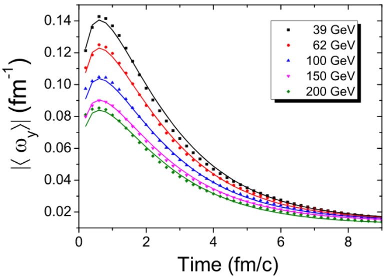

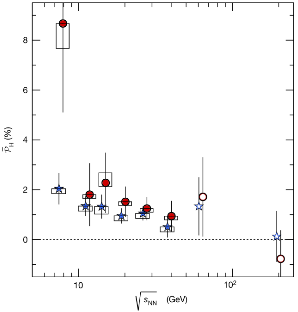

Au+Au, $b = 7$ fm

[Y. Jiang, Z.-W. Lin, and J. Liao, Phys. Rev. C **94**, 044910 (2016), arXiv:1602.06580 [hep-ph]]

$\omega \sim 0.1 - 0.2\,\text{fm}^{-1} \sim 20 - 40$ MeV

[L. Adamczyk et al. (STAR), Nature **548**, 62–65 (2017), arXiv:1701.06657 [nucl-ex]]

$\omega \sim 6$ MeV ($\sqrt{s_{NN}}$-averaged)

- How does the rotation affect to phase transitions in QCD?

Related papers

Rotation on the lattice (phase transitions were not considered):

- A. Yamamoto and Y. Hirono, Phys. Rev. Lett. **111**, 081601 (2013), arXiv:1303.6292 [hep-lat]

Related papers

Rotation on the lattice (phase transitions were not considered):

- A. Yamamoto and Y. Hirono, Phys. Rev. Lett. **111**, 081601 (2013), arXiv:1303.6292 [hep-lat]

Properties of rotating QCD matter (mostly within NJL, focused on fermions):

- S. Ebihara, K. Fukushima, and K. Mameda, Phys. Lett. B **764**, 94–99 (2017), arXiv:1608.00336 [hep-ph]
- M. Chernodub and S. Gongyo, JHEP **01**, 136 (2017), arXiv:1611.02598 [hep-th]
- X. Wang, M. Wei, Z. Li, and M. Huang, Phys. Rev. D **99**, 016018 (2019), arXiv:1808.01931 [hep-ph]
- H. Zhang, D. Hou, and J. Liao, Chin. Phys. C **44**, 111001 (2020), arXiv:1812.11787 [hep-ph]
- ...
- Y. Jiang and J. Liao, Phys. Rev. Lett. **117**, 192302 (2016), arXiv:1606.03808 [hep-ph]

Rotation suppress the chiral condensate ($S = 0$), states with $S \neq 0$ are preferable.

Related papers

Rotation on the lattice (phase transitions were not considered):

- A. Yamamoto and Y. Hirono, Phys. Rev. Lett. **111**, 081601 (2013), arXiv:1303.6292 [hep-lat]

Properties of rotating QCD matter (mostly within NJL, focused on fermions):

- S. Ebihara, K. Fukushima, and K. Mameda, Phys. Lett. B **764**, 94–99 (2017), arXiv:1608.00336 [hep-ph]
- M. Chernodub and S. Gongyo, JHEP **01**, 136 (2017), arXiv:1611.02598 [hep-th]
- X. Wang, M. Wei, Z. Li, and M. Huang, Phys. Rev. D **99**, 016018 (2019), arXiv:1808.01931 [hep-ph]
- H. Zhang, D. Hou, and J. Liao, Chin. Phys. C **44**, 111001 (2020), arXiv:1812.11787 [hep-ph]
- ...
- Y. Jiang and J. Liao, Phys. Rev. Lett. **117**, 192302 (2016), arXiv:1606.03808 [hep-ph]

Rotation suppress the chiral condensate ($S = 0$), states with $S \neq 0$ are preferable.

- Holography: X. Chen et al., (2020), arXiv:2010.14478 [hep-ph], A. A. Golubtsova, E. Gourgoulhon, and M. K. Usova, (2021), arXiv:2107.11672 [hep-th]
- Compact QED in 2+1-D M. N. Chernodub, Phys. Rev. D **103**, 054027 (2021), arXiv:2012.04924 [hep-ph]
- HRG model: Y. Fujimoto, K. Fukushima, and Y. Hidaka, Phys. Lett. B **816**, 136184 (2021), arXiv:2101.09173 [hep-ph]

Related papers

Rotation on the lattice (phase transitions were not considered):

- A. Yamamoto and Y. Hirono, Phys. Rev. Lett. **111**, 081601 (2013), arXiv:1303.6292 [hep-lat]

Properties of rotating QCD matter (mostly within NJL, focused on fermions):

- S. Ebihara, K. Fukushima, and K. Mameda, Phys. Lett. B **764**, 94–99 (2017), arXiv:1608.00336 [hep-ph]
- M. Chernodub and S. Gongyo, JHEP **01**, 136 (2017), arXiv:1611.02598 [hep-th]
- X. Wang, M. Wei, Z. Li, and M. Huang, Phys. Rev. D **99**, 016018 (2019), arXiv:1808.01931 [hep-ph]
- H. Zhang, D. Hou, and J. Liao, Chin. Phys. C **44**, 111001 (2020), arXiv:1812.11787 [hep-ph]
- ...
- Y. Jiang and J. Liao, Phys. Rev. Lett. **117**, 192302 (2016), arXiv:1606.03808 [hep-ph]

Rotation suppress the chiral condensate ($S = 0$), states with $S \neq 0$ are preferable.

- Holography: X. Chen et al., (2020), arXiv:2010.14478 [hep-ph], A. A. Golubtsova, E. Gourgoulhon, and M. K. Usova, (2021), arXiv:2107.11672 [hep-th]
- Compact QED in 2+1-D M. N. Chernodub, Phys. Rev. D **103**, 054027 (2021), arXiv:2012.04924 [hep-ph]
- HRG model: Y. Fujimoto, K. Fukushima, and Y. Hidaka, Phys. Lett. B **816**, 136184 (2021), arXiv:2101.09173 [hep-ph]

$\Rightarrow$ Critical temperature decreases due to the rotation.

Related papers

The rotation affect both gluon and quark degrees of freedom!

Related papers

The rotation affect both gluon and quark degrees of freedom!

Our lattice results for gluodynamics is opposite: critical temperature increases with rotation.

- V. V. Braguta, A. Y. Kotov, D. D. Kuznedelev, and A. A. Roenko, JETP Lett. **112**, 6–12 (2020)
- V. V. Braguta, A. Y. Kotov, D. D. Kuznedelev, and A. A. Roenko, Phys. Rev. D **103**, 094515 (2021), arXiv:2102.05084 [hep-lat]
- V. Braguta, A. Y. Kotov, D. Kuznedelev, and A. Roenko, PoS **LATTICE2021**, 125 (2022), arXiv:2110.12302 [hep-lat]

Related papers

The rotation affect both gluon and quark degrees of freedom!

Our lattice results for gluodynamics is opposite: critical temperature increases with rotation.

- V. V. Braguta, A. Y. Kotov, D. D. Kuznedelev, and A. A. Roenko, JETP Lett. **112**, 6–12 (2020)
- V. V. Braguta, A. Y. Kotov, D. D. Kuznedelev, and A. A. Roenko, Phys. Rev. D **103**, 094515 (2021), arXiv:2102.05084 [hep-lat]
- V. Braguta, A. Y. Kotov, D. Kuznedelev, and A. Roenko, PoS **LATTICE2021**, 125 (2022), arXiv:2110.12302 [hep-lat]

Taking into account the contribution of rotating gluons to NJL model:

- Y. Jiang, (2021), arXiv:2108.09622 [hep-ph]

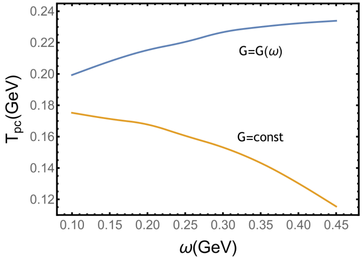

The running effective coupling $G(\omega)$ is introduced.

$\Rightarrow$ Critical temperature increases due to the rotation.

Rotating reference frame

- QCD (at thermal equilibrium) is investigated in the reference frame which rotates with the system with angular velocity Ω .
- In this reference frame there appears an external gravitational field

$$g_{\mu\nu} = \begin{pmatrix} 1 - r^2\Omega^2 & \Omega y & -\Omega x & 0 \\ \Omega y & -1 & 0 & 0 \\ -\Omega x & 0 & -1 & 0 \\ 0 & 0 & 0 & -1 \end{pmatrix} .$$

[1] A. Yamamoto and Y. Hirono, Phys. Rev. Lett. **111**, 081601 (2013), arXiv:1303.6292 [hep-lat].

Rotating reference frame

- QCD (at thermal equilibrium) is investigated in the reference frame which rotates with the system with angular velocity Ω .
- In this reference frame there appears an external gravitational field

$$g_{\mu\nu} = \begin{pmatrix} 1 - r^2\Omega^2 & \Omega y & -\Omega x & 0 \\ \Omega y & -1 & 0 & 0 \\ -\Omega x & 0 & -1 & 0 \\ 0 & 0 & 0 & -1 \end{pmatrix} .$$

- Tolman-Ehrenfest effect: In gravitational field the temperature isn't a constant in space at thermal equilibrium:

$$T(r)\sqrt{1 - r^2\Omega^2} = const \equiv T ,$$

One could expect, that the rotation effectively warm up the periphery and as a result, from kinematics, the critical temperature should decreases.

[1] A. Yamamoto and Y. Hirono, Phys. Rev. Lett. **111**, 081601 (2013), arXiv:1303.6292 [hep-lat].

Rotating reference frame

- QCD (at thermal equilibrium) is investigated in the reference frame which rotates with the system with angular velocity Ω .
- In this reference frame there appears an external gravitational field

$$g_{\mu\nu} = \begin{pmatrix} 1 - r^2\Omega^2 & \Omega y & -\Omega x & 0 \\ \Omega y & -1 & 0 & 0 \\ -\Omega x & 0 & -1 & 0 \\ 0 & 0 & 0 & -1 \end{pmatrix} .$$

- Tolman-Ehrenfest effect: In gravitational field the temperature isn't a constant in space at thermal equilibrium:

$$T(r)\sqrt{1 - r^2\Omega^2} = const \equiv T \,,$$

One could expect, that the rotation effectively warm up the periphery and as a result, from kinematics, the critical temperature should decreases.

- The partition function is[1]

$$Z = \int D\psi\, D\bar{\psi}\, DA \, \exp\left(- S_G[A, \Omega] - S_F[\bar{\psi}, \psi, A, \Omega] \right) . \tag{1}$$

[1] A. Yamamoto and Y. Hirono, Phys. Rev. Lett. **111**, 081601 (2013), arXiv:1303.6292 [hep-lat].

Rotating QCD: continuum action

The Euclidean gluon action can be written as

$$S_G = \frac{1}{4g^2} \int d^4x \sqrt{g_E}\, g_E^{\mu\nu} g_E^{\alpha\beta} F^a_{\mu\alpha} F^a_{\nu\beta}\,. \tag{2}$$

And the quark action reads as follows[2]

$$S_F = \int d^4x \sqrt{g_E}\, \bar\psi \big(\gamma^\mu (D_\mu - \Gamma_\mu) + m\big)\psi\,, \tag{3}$$

The covariant derivative D_μ and spinor affine connection Γ_μ is

$$D_\mu = \partial_\mu - iA_\mu\,, \tag{4}$$

$$\Gamma_\mu = -\frac{i}{4}\sigma^{ij}\omega_{\mu ij}\,, \tag{5}$$

$$\sigma^{ij} = \frac{i}{2}(\gamma^i\gamma^j - \gamma^j\gamma^i) \tag{6}$$

$$\omega_{\mu ij} = g^E_{\alpha\beta} e^\alpha_i (\partial_\mu e^\beta_j + \Gamma^\beta_{\nu\mu} e^\nu_j) \tag{7}$$

where e^μ_i is the vierbein and $\Gamma^\alpha_{\mu\nu}$ is the Christoffel symbol.

[2] A. Yamamoto and Y. Hirono, Phys. Rev. Lett. **111**, 081601 (2013), arXiv:1303.6292 [hep-lat].

Rotating QCD: continuum gluon action

The Euclidean metric tensor can be obtained from $g_{\mu\nu}$ by Wick rotation $t \to i\tau$

$$g^E_{\mu\nu} = \begin{pmatrix} 1 & 0 & 0 & y\Omega_I \\ 0 & 1 & 0 & -x\Omega_I \\ 0 & 0 & 1 & 0 \\ y\Omega_I & -x\Omega_I & 0 & 1 + r^2\Omega_I^2 \end{pmatrix},$$

where imaginary angular velocity $\Omega_I = -i\Omega$ is introduced.

Rotating QCD: continuum gluon action

The Euclidean metric tensor can be obtained from $g_{\mu\nu}$ by Wick rotation $t \to i\tau$

$$g^E_{\mu\nu} = \begin{pmatrix} 1 & 0 & 0 & y\Omega_I \\ 0 & 1 & 0 & -x\Omega_I \\ 0 & 0 & 1 & 0 \\ y\Omega_I & -x\Omega_I & 0 & 1 + r^2\Omega_I^2 \end{pmatrix},$$

where imaginary angular velocity $\Omega_I = -i\Omega$ is introduced. Substituting the $(g_E)_{\mu\nu}$ to formula (8) one gets

$$S_G = \frac{1}{2g^2} \int d^4x \, \Big[(1 + r^2\Omega_I^2) F^a_{xy} F^a_{xy} + (1 + y^2\Omega_I^2) F^a_{xz} F^a_{xz} + (1 + x^2\Omega_I^2) F^a_{yz} F^a_{yz} + \\ + F^a_{x\tau} F^a_{x\tau} + F^a_{y\tau} F^a_{y\tau} + F^a_{z\tau} F^a_{z\tau} - \\ + 2y\Omega_I (F^a_{xy} F^a_{y\tau} + F^a_{xz} F^a_{z\tau}) - 2x\Omega_I (F^a_{yx} F^a_{x\tau} + F^a_{yz} F^a_{z\tau}) + 2xy\Omega_I^2 F^a_{xz} F^a_{zy} \Big].$$

Rotating QCD: continuum gluon action

The Euclidean metric tensor can be obtained from $g_{\mu\nu}$ by Wick rotation $t \to i\tau$

$$g^E_{\mu\nu} = \begin{pmatrix} 1 & 0 & 0 & y\Omega_I \\ 0 & 1 & 0 & -x\Omega_I \\ 0 & 0 & 1 & 0 \\ y\Omega_I & -x\Omega_I & 0 & 1 + r^2\Omega_I^2 \end{pmatrix},$$

where imaginary angular velocity $\Omega_I = -i\Omega$ is introduced. Substituting the $(g_E)_{\mu\nu}$ to formula (8) one gets

$$S_G = \frac{1}{2g^2}\int d^4x \Big[(1 + r^2\Omega_I^2) F^a_{xy}F^a_{xy} + (1 + y^2\Omega_I^2) F^a_{xz}F^a_{xz} + (1 + x^2\Omega_I^2) F^a_{yz}F^a_{yz} + \\ + F^a_{x\tau}F^a_{x\tau} + F^a_{y\tau}F^a_{y\tau} + F^a_{z\tau}F^a_{z\tau} - \\ + 2y\Omega_I (F^a_{xy}F^a_{y\tau} + F^a_{xz}F^a_{z\tau}) - 2x\Omega_I (F^a_{yx}F^a_{x\tau} + F^a_{yz}F^a_{z\tau}) + 2xy\Omega_I^2 F^a_{xz}F^a_{zy} \Big].$$

Sign problem

- The Euclidean action is complex-valued function with real rotation!
- The Monte–Carlo simulations are conducted with imaginary angular velocity $\Omega_I = -i\Omega$.
- The results are analytically continued to the region of the real angular velocity.

The covariant Dirac operator depends on the choice of the vierbein. We choose the vierbein in the form[3]

$$e^x_1 = e^y_2 = e^z_3 = e^\tau_4 = 1\,, \quad e^x_4 = -y\Omega_I\,, \quad e^y_4 = x\Omega_I\,, \quad \text{and other } e^\mu_i = 0$$

As the result, the Euclidean quark action is

$$S_F = \int d^4x\,\bar\psi\left(\gamma^x D_x + \gamma^y D_y + \gamma^z D_z + \gamma^\tau\left(D_\tau + i\Omega_I\frac{\sigma^{12}}{2}\right) + m\right)\psi\,, \tag{8}$$

where the gamma matrices are given by $\gamma^\mu = \gamma^i e^\mu_i$

$$\gamma^x = \gamma^1 - y\Omega_I\gamma^4\,, \quad \gamma^y = \gamma^2 + x\Omega_I\gamma^4\,, \quad \gamma^z = \gamma^3\,, \quad \gamma^\tau = \gamma^4\,. \tag{9}$$

[3] A. Yamamoto and Y. Hirono, Phys. Rev. Lett. **111**, 081601 (2013), arXiv:1303.6292 [hep-lat].

Rotating QCD: continuum quark action

The covariant Dirac operator depends on the choice of the vierbein. We choose the vierbein in the form[3]

$$e^x_1 = e^y_2 = e^z_3 = e^\tau_4 = 1\,, \quad e^x_4 = -y\Omega_I\,, \quad e^y_4 = x\Omega_I\,, \quad \text{and other } e^\mu_i = 0$$

As the result, the Euclidean quark action is

$$S_F = \int d^4x\,\bar\psi\left(\gamma^x D_x + \gamma^y D_y + \gamma^z D_z + \gamma^\tau\left(D_\tau + i\Omega_I\frac{\sigma^{12}}{2}\right) + m\right)\psi\,, \qquad (8)$$

where the gamma matrices are given by $\gamma^\mu = \gamma^i e^\mu_i$

$$\gamma^x = \gamma^1 - y\Omega_I\gamma^4\,, \quad \gamma^y = \gamma^2 + x\Omega_I\gamma^4\,, \quad \gamma^z = \gamma^3\,, \quad \gamma^\tau = \gamma^4\,. \qquad (9)$$

The quark action contains orbit-rotation coupling term $\gamma^\tau\Omega_I(xD_y - yD_x)$ and spin-rotation coupling term $i\gamma^\tau\Omega_I\sigma^{12}/2$.

[3] A. Yamamoto and Y. Hirono, Phys. Rev. Lett. **111**, 081601 (2013), arXiv:1303.6292 [hep-lat].

Rotating QCD: continuum quark action

The covariant Dirac operator depends on the choice of the vierbein. We choose the vierbein in the form[3]

$$e_1^x = e_2^y = e_3^z = e_4^\tau = 1\,, \quad e_4^x = -y\Omega_I\,, \quad e_4^y = x\Omega_I\,, \quad \text{and other } e_i^\mu = 0$$

As the result, the Euclidean quark action is

$$S_F = \int d^4x\, \bar{\psi}\left(\gamma^x D_x + \gamma^y D_y + \gamma^z D_z + \gamma^\tau \left(D_\tau + i\Omega_I \frac{\sigma^{12}}{2}\right) + m\right)\psi\,, \tag{8}$$

where the gamma matrices are given by $\gamma^\mu = \gamma^i e_i^\mu$

$$\gamma^x = \gamma^1 - y\Omega_I\gamma^4\,, \quad \gamma^y = \gamma^2 + x\Omega_I\gamma^4\,, \quad \gamma^z = \gamma^3\,, \quad \gamma^\tau = \gamma^4\,. \tag{9}$$

The quark action contains orbit-rotation coupling term $\gamma^\tau\Omega_I(xD_y - yD_x)$ and spin-rotation coupling term $i\gamma^\tau\Omega_I\sigma^{12}/2$.

Sign problem

- The Euclidean action is complex-valued function with real rotation!

[3] A. Yamamoto and Y. Hirono, Phys. Rev. Lett. 111, 081601 (2013), arXiv:1303.6292 [hep-lat].

We use RG-improved (Iwasaki) lattice gauge action (for non-rotating part):

$$S_G = \beta \sum_x \Big((c_0 + r^2\Omega_I^2) W_{xy}^{1\times1} + (c_0 + y^2\Omega_I^2) W_{xz}^{1\times1} + (c_0 + x^2\Omega_I^2) W_{yz}^{1\times1} + \\ + c_0 \big(W_{x\tau}^{1\times1} + W_{y\tau}^{1\times1} + W_{z\tau}^{1\times1}\big) + y\Omega_I \big(W_{xy\tau}^{1\times1\times1} + W_{xz\tau}^{1\times1\times1}\big) - \\ - x\Omega_I \big(W_{yx\tau}^{1\times1\times1} + W_{yz\tau}^{1\times1\times1}\big) + xy\Omega_I^2 W_{xzy}^{1\times1\times1} + \sum_{\mu\neq\nu} c_1 W_{\mu\nu}^{1\times2} \Big)\,, \qquad (10)$$

with $\beta = 6/g^2$, and $c_0 = 1 - 8c_1$, and $c_1 = -0.331$, where

$$W_{\mu\nu}^{1\times1}(x) = 1 - \frac{1}{3}\mathrm{Re\ Tr}\ \bar{U}_{\mu\nu}(x)\,, \qquad (11)$$

$$W_{\mu\nu}^{1\times2}(x) = 1 - \frac{1}{3}\mathrm{Re\ Tr}\ R_{\mu\nu}(x)\,, \qquad (12)$$

$$W_{\mu\nu\rho}^{1\times1\times1}(x) = -\frac{1}{3}\mathrm{Re\ Tr}\ \bar{V}_{\mu\nu\rho}(x)\,, \qquad (13)$$

$\bar{U}_{\mu\nu}$ denotes clover-type average of 4 plaquettes,

$R_{\mu\nu}$ is a rectangular loop,

$\bar{V}_{\mu\nu\rho}$ is asymmetric chair-type average of 8 chairs.

Rotating QCD: gluon lattice action

We use RG-improved (Iwasaki) lattice gauge action (for non-rotating part):

$$S_G = \beta \sum_x \Big((c_0 + r^2\Omega_I^2) W_{xy}^{1\times1} + (c_0 + y^2\Omega_I^2) W_{xz}^{1\times1} + (c_0 + x^2\Omega_I^2) W_{yz}^{1\times1} + \\ + c_0 \left(W_{x\tau}^{1\times1} + W_{y\tau}^{1\times1} + W_{z\tau}^{1\times1} \right) + y\Omega_I \left(W_{xy\tau}^{1\times1\times1} + W_{xz\tau}^{1\times1\times1} \right) - \\ - x\Omega_I \left(W_{yx\tau}^{1\times1\times1} + W_{yz\tau}^{1\times1\times1} \right) + xy\Omega_I^2 W_{xzy}^{1\times1\times1} + \sum_{\mu\neq\nu} c_1 W_{\mu\nu}^{1\times2} \Big) , \quad (10)$$

with $\beta = 6/g^2$, and $c_0 = 1 - 8c_1$, and $c_1 = -0.331$, where

$$W_{\mu\nu}^{1\times1}(x) = 1 - \frac{1}{3}\mathrm{Re\ Tr\ } \bar{U}_{\mu\nu}(x) , \quad (11)$$

$$W_{\mu\nu}^{1\times2}(x) = 1 - \frac{1}{3}\mathrm{Re\ Tr\ } R_{\mu\nu}(x) , \quad (12)$$

$$W_{\mu\nu\rho}^{1\times1\times1}(x) = -\frac{1}{3}\mathrm{Re\ Tr\ } \bar{V}_{\mu\nu\rho}(x) , \quad (13)$$

$\bar{U}_{\mu\nu}$ denotes clover-type average of 4 plaquettes,

$R_{\mu\nu}$ is a rectangular loop,

$\bar{V}_{\mu\nu\rho}$ is asymmetric chair-type average of 8 chairs.

The lattice quark action has the following form ($N_f = 2$ clover-improved Wilson fermions are used)

$$S_F = \sum_f \sum_{x_1,x_2} \bar{\psi}^f(x_1) \Big\{ \delta_{x_1,x_2} - \kappa \Big[(1-\gamma^x)T_{x+} + (1+\gamma^x)T_{x-} + (1-\gamma^y)T_{y+} + (1+\gamma^y)T_{y-} + (1-\gamma^z)T_{z+} + (1+\gamma^z)T_{z-} + (1-\gamma^\tau)\exp\left(ia\Omega_I \frac{\sigma^{12}}{2}\right)T_{\tau+} + (1+\gamma^\tau)\exp\left(-ia\Omega_I \frac{\sigma^{12}}{2}\right)T_{\tau-} \Big] - \delta_{x_1,x_2} c_{SW}\kappa \sum_{\mu<\nu} \sigma_{\mu\nu}F_{\mu\nu} \Big\} \psi^f(x_2), \quad (14)$$

where $\kappa = 1/(8+2am)$, $T_{\mu+} = U_\mu(x_1)\delta_{x_1+\mu,x_2}$, $T_{\mu-} = U^\dagger_\mu(x_1)\delta_{x_1-\mu,x_2}$ and

$$\gamma^x = \gamma^1 - y\Omega_I\gamma^4, \quad \gamma^y = \gamma^2 + x\Omega_I\gamma^4, \quad \gamma^z = \gamma^3, \quad \gamma^\tau = \gamma^4.$$

The clover coefficient is taken as $c_{SW} = (1 - W^{1\times1})^{-3/4} = (1 - 0.8412/\beta)^{-3/4}$ (one-loop result for the plaquette are used).

The spin-rotation coupling term is exponentiated like chemical potential.

Rotating QCD: quark lattice action

The lattice quark action has the following form ($N_f = 2$ clover-improved Wilson fermions are used)

$$S_F = \sum_f \sum_{x_1,x_2} \bar{\psi}^f(x_1) \Bigg\{ \delta_{x_1,x_2} - \kappa \Big[(1-\gamma^x) T_{x+} + (1+\gamma^x) T_{x-} + (1-\gamma^y) T_{y+} + (1+\gamma^y) T_{y-} + (1-\gamma^z) T_{z+} + (1+\gamma^z) T_{z-} + (1-\gamma^\tau) \exp\left(ia\Omega_I \frac{\sigma^{12}}{2} \right) T_{\tau+} + (1+\gamma^\tau) \exp\left(-ia\Omega_I \frac{\sigma^{12}}{2} \right) T_{\tau-} \Big] - \delta_{x_1,x_2} c_{SW} \kappa \sum_{\mu<\nu} \sigma_{\mu\nu} F_{\mu\nu} \Bigg\} \psi^f(x_2), \quad (14)$$

where $\kappa = 1/(8+2am)$, $T_{\mu+} = U_\mu(x_1)\delta_{x_1+\mu,x_2}$, $T_{\mu-} = U^\dagger_\mu(x_1)\delta_{x_1-\mu,x_2}$ and

$$\gamma^x = \gamma^1 - y\Omega_I\gamma^4, \quad \gamma^y = \gamma^2 + x\Omega_I\gamma^4, \quad \gamma^z = \gamma^3, \quad \gamma^\tau = \gamma^4.$$

The clover coefficient is taken as $c_{SW} = (1 - W^{1\times1})^{-3/4} = (1 - 0.8412/\beta)^{-3/4}$ (one-loop result for the plaquette are used).

The spin-rotation coupling term is exponentiated like chemical potential.

The resulting partition function is

$$Z = \int D\psi\, D\bar{\psi}\, DU \;\exp\big(-S_G[U,\Omega_I] - S_F[\bar{\psi},\psi,m,U,\Omega_I]\big) = \\ = \int DU \;\det M[m,U,\Omega_I]\; e^{(-S_G[U,\Omega_I])} \qquad (15)$$

- The rotation affect both gluon and quark degrees of freedom!
- Simulation is performed on the lattice $N_t \times N_z \times N_s^2$ $(N_s = N_x = N_y)$, which rotates around z-axis.
- $N_f = 2$ clover-improved Wilson fermions + RG-improved (Iwasaki) gauge action are used.
- "Replay" trick[4] is enabled to increase the stability of the HMC-algorithm.
- We reanalyze data for $m_{PS}a$ and $m_V a$ at zero temperature from CP-PACS and WHOT-QCD collaborations to restore LCP's and set the scale.

[4] A. D. Kennedy, Nucl. Phys. B Proc. Suppl. **140**, edited by G. T. Bodwin et al., 190–203 (2005), arXiv:hep-lat/0409167.

LCP and scale setting

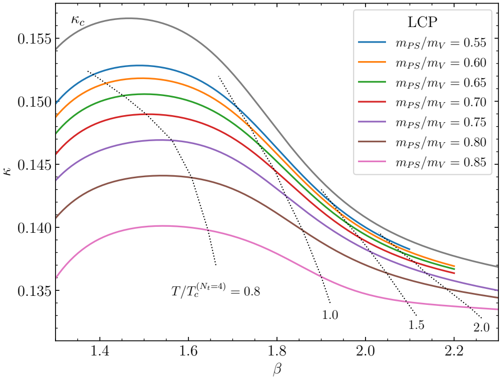

To set the temperature along the given LCP we use the zero-temperature mass of vector meson (m_V-input)

$$\frac{T}{m_V}(m_{PS}/m_V, \beta) = \frac{1}{N_t \times m_V a(m_{PS}/m_V, \beta)}\,. \tag{16}$$

and find

$$\frac{T}{T_{pc}}(\beta) = \frac{m_V a(\beta_{pc,\Omega=0})}{m_V a(\beta)}$$

- The system should be limited in the directions, which are orthogonal to the rotation axis: $\Omega_I (N_s - 1)a/\sqrt{2} < 1$

- The system should be limited in the directions, which are orthogonal to the rotation axis: $\Omega_I(N_s - 1)a/\sqrt{2} < 1$

$$\Downarrow$$

- The boundary conditions in directions x, y have to be treated carefully! The results depend on BC for any approach.
- The use of periodic/open/Dirichlet BC gives qualitatively the same results for rotating gluodynamics. Up to now, PBC in directions x, y have been imposed.
- The critical temperature in gluodynamics depends mainly on the linear velocity on the boundary $v_I = \Omega_I(N_s - 1)a$. Thus, v_I is fixed in simulations instead of angular velocity Ω_I in physical units (e.g., MeV).

The lattice version of Polyakov loop is defined as usual:

$$L(\vec{x}) = \mathrm{Tr}\left[\prod_{\tau=0}^{N_t-1} U_4(\vec{x},\tau)\right], \qquad L = \frac{1}{N_s^2 N_z}\sum_{\vec{x}} L(\vec{x}). \tag{17}$$

The pseudo-critical temperature T_{pc} is determined using the Polyakov loop susceptibility

$$\chi = N_s^2 N_z \left(\langle |L|^2\rangle - \langle |L|\rangle^2\right), \tag{18}$$

by means of the Gaussian fit and as inflection point of Polyakov loop.

The Polyakov loop is not an order parameter in QCD, but it still rapidly changes from confinement to deconfinement phase. The chiral transition also appears.

- In confinement phase $\langle L\rangle$ is less than in deconfinement phase.
- In chirally broken phase $\langle\bar{\psi}\psi\rangle$ is greater than in chirally restored phase.

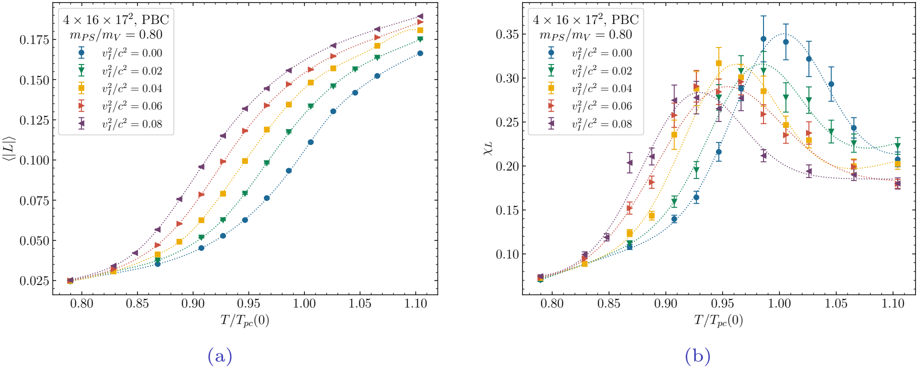

Figure: The Polyakov loop (a) and the Polyakov loop susceptibility (b) as a function of $T/T_{pc}(\Omega = 0)$ for different values of imaginary linear velocity on the boundary v_I. Lattice $4 \times 16 \times 17^2$, LCP $m_{PS}/m_V = 0.80$.

- Pseudo-critical temperature decreases due to imaginary rotation (same as in gluodynamics).

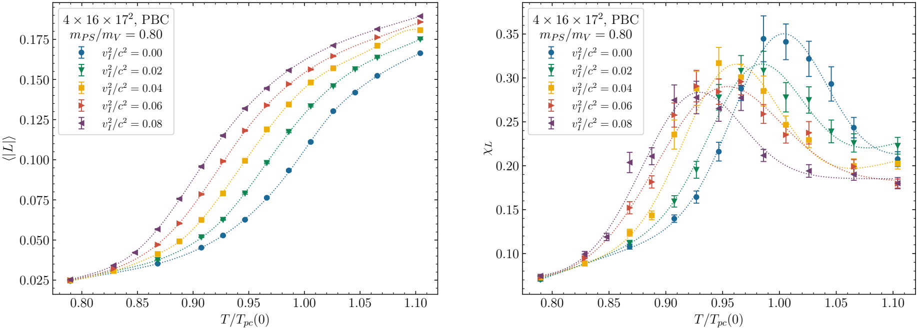

(a) (b)

Figure: The Polyakov loop (a) and the Polyakov loop susceptibility (b) as a function of $T/T_{pc}(\Omega = 0)$ for different values of imaginary linear velocity on the boundary v_I. Lattice $4 \times 16 \times 17^2$, LCP $m_{PS}/m_V = 0.80$.

- Pseudo-critical temperature decreases due to imaginary rotation (same as in gluodynamics).

One can rewrite the full action as $S_G(\Omega_G) + S_F(\Omega_F)$ and rotate each part separately!

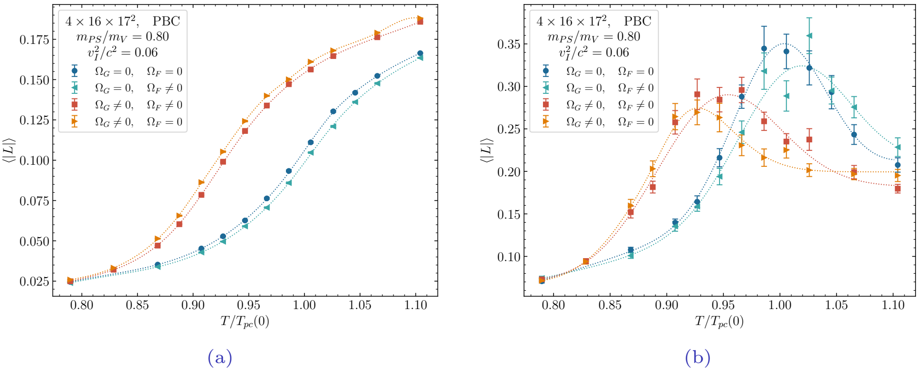

Figure: The Polyakov loop (a) and the Polyakov loop susceptibility (b) as a function of T/T_{pc} for various rotation regimes. Lattice $4 \times 16 \times 17^2$, $m_{PS}/m_V = 0.80$.

Rotating QCD: various rotation regimes

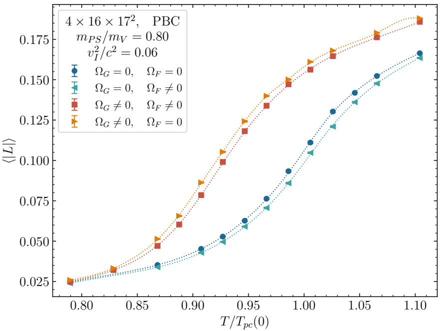

(a)

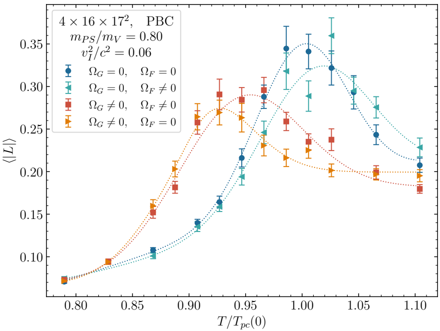

(b)

Figure: The Polyakov loop (a) and the Polyakov loop susceptibility (b) as a function of T/T_{pc} for various rotation regimes. Lattice $4 \times 16 \times 17^2$, $m_{PS}/m_V = 0.80$.

- Rotation of fermions and gluons separately has the opposite influence on the critical temperature.

Rotating QCD: various rotation regimes

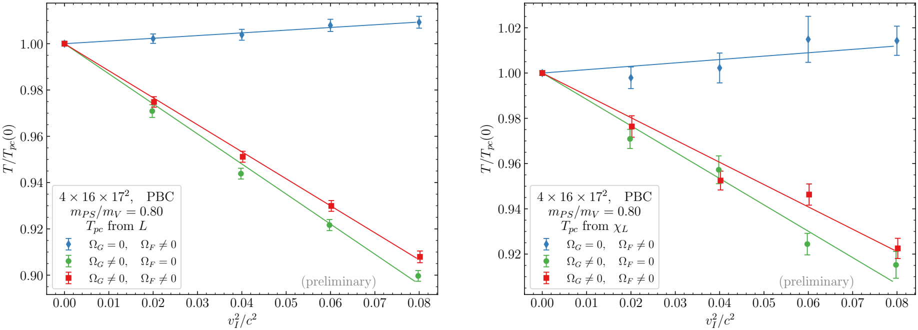

Figure: The pseudo-critical temperature as a function of imaginary linear velocity on the boundary for various rotation regimes (full, only gluons, only fermions).

$$\frac{T_{pc}(v_I)}{T_{pc}(0)} = 1 - B_2 \frac{v_I^2}{c^2} \tag{19}$$

$\Omega_G = \Omega_F \neq 0$	$\Omega_G \neq 0$	$\Omega_F \neq 0$
$B_2 > 0$	$B_2^{(G)} > B_2$	$B_2^{(F)} < 0$

Rotating QCD: critical temperature

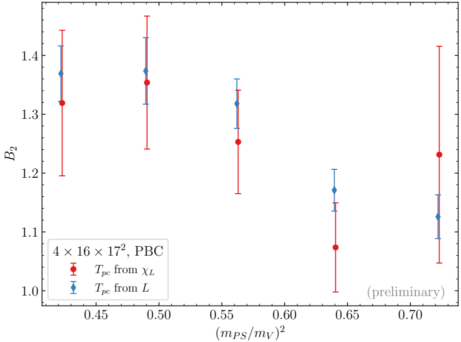

LCP's with $m_{PS}/m_V = 0.65, 0.70, 0.75, 0.80, 0.85$ were considered.

$$\frac{T_{pc}(v_I)}{T_{pc}(0)} = 1 - B_2 \frac{v_I^2}{c^2}$$

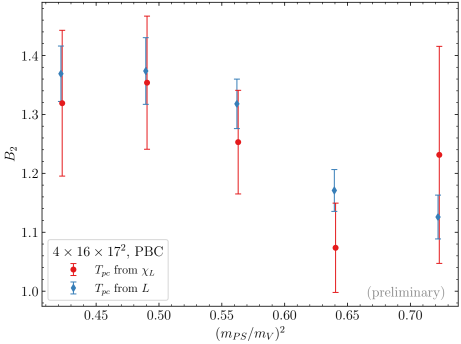

LCP's with $m_{PS}/m_V = 0.65, 0.70, 0.75, 0.80, 0.85$ were considered.

$$\frac{T_{pc}(v_I)}{T_{pc}(0)} = 1 - B_2 \frac{v_I^2}{c^2} \qquad \Longrightarrow \qquad \frac{T_{pc}(v)}{T_{pc}(0)} = 1 + B_2 \frac{v^2}{c^2}$$

- The pseudo-critical temperature increases with the angular velocity ($v \propto \Omega$).
- The coefficient B_2 just slightly depends on the pion mass in considered range.
- The chiral transition shifts to the same direction as confinement-deconfinement transition.

Conclusions

- The separate rotation of quarks and gluons in QCD has the opposite influence on the critical temperature.
- The critical temperature in QCD increases with angular velocity ($v \propto \Omega$)

$$\frac{T_{pc}(v)}{T_{pc}(0)} = 1 + B_2 \frac{v^2}{c^2} \,.$$

  It's not Tolman-Ehrenfest effect!
- The coefficient B_2 just slightly depends on the pion mass in considered range ($m_{PS}/m_V = 0.65 \ \ldots \ 0.85$).
- The results are similar to gluodynamics, where the critical temperature also increases with angular velocity.
- It should be noted, that NJL (and other phenomenological models) predicts that critical temperature decreases due to the rotation. But taking into account the contribution of rotating gluons leads to an increase in T_c.

- Future plans: increase statistics; simulations with smaller pion mass, on finer lattices ($N_t = 6, 8$), with an open BC.

Thank you for your attention!

Rotating QCD; Wilson gauge action + Wilson fermions

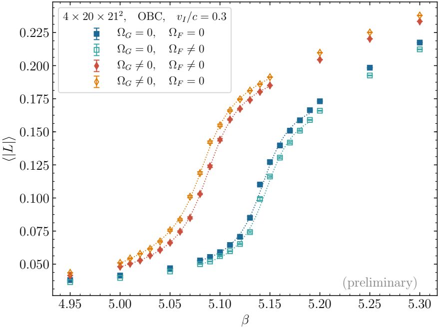

(a)

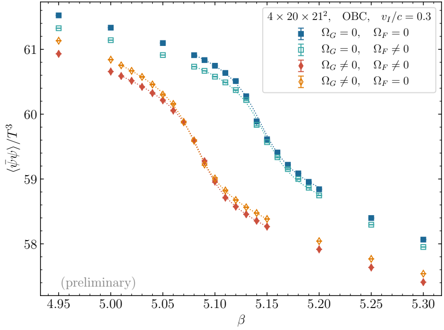

(b)

Figure: The Polyakov loop (a) and the (unrenormalized!) chiral condensate (b) as a function of β for different values of imaginary angular velocity Ω_I. Lattice $4 \times 20 \times 21^2$, the hopping parameter $\kappa = 0.170$.

- Rotation of fermions and gluons separately has the opposite influence on the critical coupling (temperature), $N_f = 2$ Wilson fermions.

Rotating QCD; Wilson gauge action + Wilson fermions

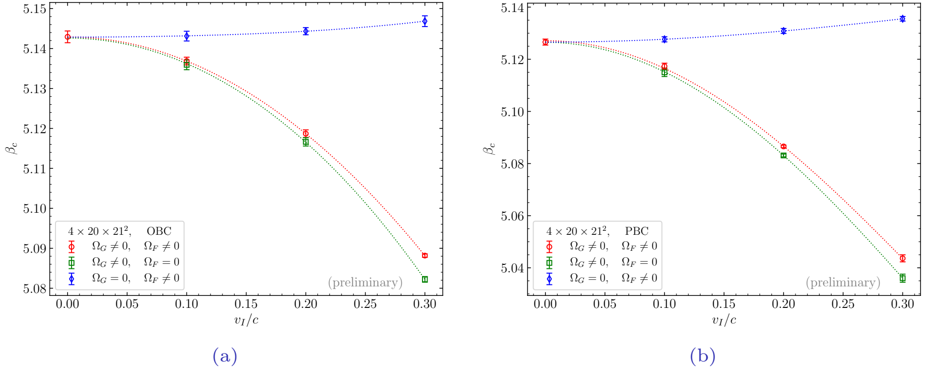

Figure: The critical value β_c as function of imaginary linear velocity on the boundary; $N_f = 2$ Wilson fermions, $\kappa = 1.70$, result of β-scan.

- Rotation of fermions and gluons separately has the opposite influence on the critical coupling (temperature).
- The results are qualitatively the same for OBC and PBC.

Critical temperature; Iwasaki + clover-improved Wilson fermions

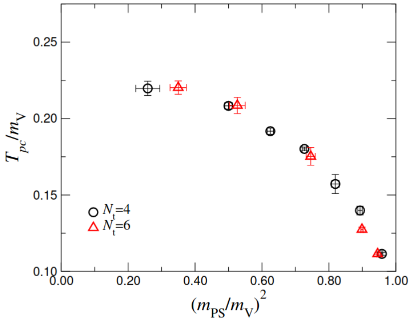

In chiral limit $T_{pc}/m_V \sim 0.21 - 0.23, \quad T_{pc} \sim 160 - 180$ MeV

S. Ejiri et al. (WHOT-QCD), Phys. Rev. D **82**, 014508 (2010), arXiv:0909.2121 [hep-lat]

Masses of light mesons; Iwasaki + clover-improved Wilson fermions

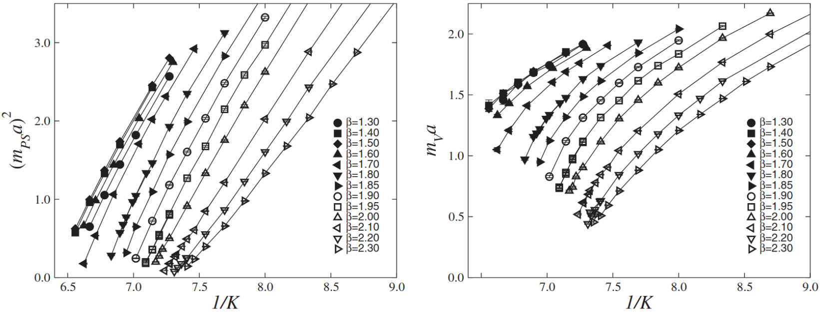

Figure from Y. Maezawa et al. (WHOT-QCD), Phys. Rev. D **75**, 074501 (2007), arXiv:hep-lat/0702004

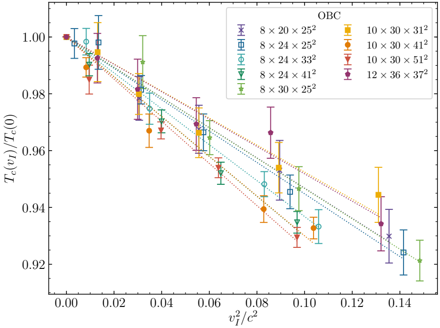

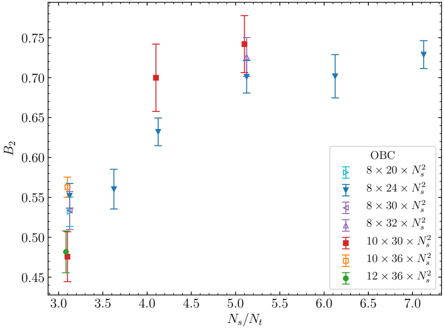

The linear velocity on the boundary $v_I = \Omega_I \, (N_s - 1) \, a(\beta_c)/2$

$$\frac{T_c(v_I)}{T_c(0)} = 1 - B_2 \frac{v_I^2}{c^2} \qquad \Longrightarrow \qquad \frac{T_c(v)}{T_c(0)} = 1 + B_2 \frac{v^2}{c^2}$$

- The critical temperature increases with the angular velocity.
- The coefficient B_2 slightly depends on the transverse lattice size (N_s/N_t), but it is almost independent of both the lattice spacing and the lattice size along the rotation axis (N_z/N_t).
- For lattices with sufficiently large N_s and OBC the coefficient is $B_2 \simeq 0.7$.

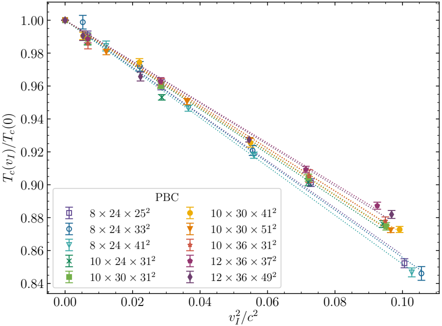

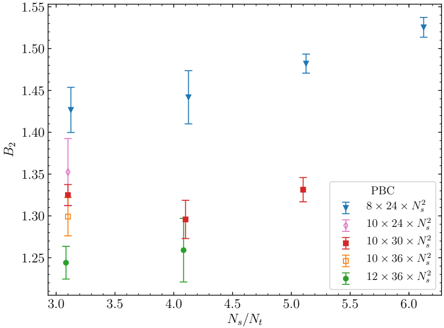

The linear velocity on the boundary $v_I = \Omega_I\,(N_s - 1)\,a(\beta_c)/2$

$$\frac{T_c(v_I)}{T_c(0)} = 1 - B_2\frac{v_I^2}{c^2} \qquad \Longrightarrow \qquad \frac{T_c(v)}{T_c(0)} = 1 + B_2\frac{v^2}{c^2}$$

- The critical temperature increases with the angular velocity.
- The results for the finest lattices with $N_t = 10, 12$ are close to each others, and for PBC the coefficient is $B_2 \sim 1.3$.

Rotating gluodynamics: Dirichlet boundary conditions

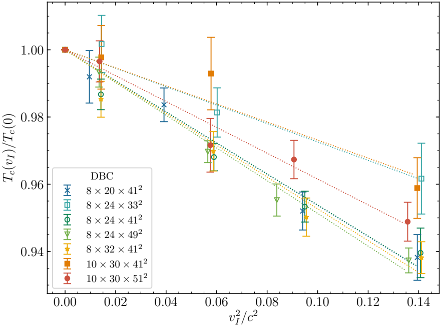

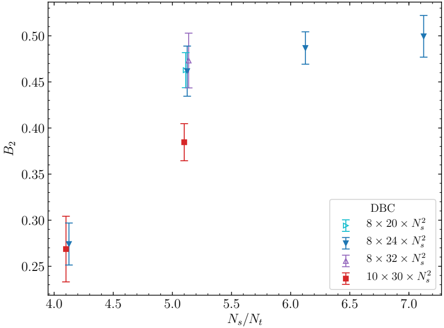

The linear velocity on the boundary $v_I = \Omega_I\,(N_s - 1)\,a(\beta_c)/2$

$$\frac{T_c(v_I)}{T_c(0)} = 1 - B_2 \frac{v_I^2}{c^2} \qquad \Longrightarrow \qquad \frac{T_c(v)}{T_c(0)} = 1 + B_2 \frac{v^2}{c^2}$$

- The critical temperature increases with the angular velocity.
- For lattices with sufficiently large N_s and DBC the coefficient goes to plateau $B_2 \sim 0.5$.